



OPEN ACCESS

EDITED BY

Raghvendra Ashok Bohara,
University of Galway, Ireland

REVIEWED BY

Miguel Angel Mateos Timoneda,
International University of Catalonia,
Spain
Amir Alsharabasy,
University of Galway, Ireland

*CORRESPONDENCE

Arturo E. Aguilar-Rabiela,
aguilar.rabiela@exatec.tec.mx
Aldo R. Boccaccini,
aldo.boccaccini@fau.de

SPECIALTY SECTION

This article was submitted to Bioinspired
and Complex Materials,
a section of the journal
Frontiers in Biomaterials Science

RECEIVED 23 May 2022

ACCEPTED 24 November 2022

PUBLISHED 05 December 2022

CITATION

Aguilar-Rabiela AE, Unterweger H,
Alexiou C and Boccaccini AR (2022),
Reduction of the *in vitro* toxicity of
elevated concentrations of SPION^{LA} by
its administration through PHBV/
curcumin composite microspheres.
Front. Front. Biomater. Sci. 1:951343.
doi: 10.3389/fbiom.2022.951343

COPYRIGHT

© 2022 Aguilar-Rabiela, Unterweger,
Alexiou and Boccaccini. This is an open-
access article distributed under the
terms of the [Creative Commons
Attribution License \(CC BY\)](https://creativecommons.org/licenses/by/4.0/). The use,
distribution or reproduction in other
forums is permitted, provided the
original author(s) and the copyright
owner(s) are credited and that the
original publication in this journal is
cited, in accordance with accepted
academic practice. No use, distribution
or reproduction is permitted which does
not comply with these terms.

Reduction of the *in vitro* toxicity of elevated concentrations of SPION^{LA} by its administration through PHBV/curcumin composite microspheres

Arturo E. Aguilar-Rabiela^{1,2,3*}, Harald Unterweger⁴,
Christoph Alexiou⁴ and Aldo R. Boccaccini^{1*}

¹Institute of Biomaterials, Department of Materials Science and Engineering, University of Erlangen-Nuremberg, Erlangen, Germany, ²Escuela de Ingeniería y Ciencias, Tecnológico de Monterrey, Atizapán de Zaragoza, Estado de México, Mexico, ³Tissue Engineering Research Group, Department of Anatomy & Regenerative Medicine, Royal College of Surgeons in Ireland (RCSI), Dublin, Ireland, ⁴Department of Otorhinolaryngology, Head and Neck Surgery, Section of Experimental Oncology and Nanomedicine (SEON), Else Kröner-Fresenius-Stiftung Professorship, University Hospital Erlangen, Erlangen, Germany

Superparamagnetic iron oxide nanoparticles have been developed for various biomedical applications for decades. In this work, lauric acid-coated SPION (SPION^{LA}) were incorporated into poly (3-hydroxybutyrate-co-3-hydroxyvalerate) (PHBV) at different ratios to produce composite microspheres, which were evaluated for their properties, including potential cytotoxicity. Additionally, a phytotherapeutic extract, curcumin, was loaded into the resulting microspheres to develop magnetic drug delivery capsules. The results show a significant improvement in the cytocompatibility after 7 days of SPION^{LA} administrated in cells through the composite microspheres compared to pristine SPION^{LA}. The composite also exhibited prolonged cumulative release of curcumin in a simulated body fluid environment. The results confirmed the efficacy of the mixture of PHBV and curcumin in attenuating potential side effects due to direct administration of high initial amounts of SPION^{LA} while maintaining magnetic properties in the resulting composite. The results add evidence to the potential of these composite devices for targeted drug delivery applications.

KEYWORDS

SPIONs, composite microspheres, targeted drug delivery, controlled release, PHBV

Introduction

Superparamagnetic Iron Oxide Nanoparticles (SPIONs) are increasingly being explored for a variety of medical applications (Chomoucka et al., 2010; Mok and Zhang, 2013; Matuszak et al., 2015). One, in particular, is the possibility to enable targeted drug delivery. This could be very useful in developing alternative cancer treatments in which the release occurs mainly in the specific cancerous tissues, thus

reducing undesirable effects in healthy tissues (Nigmatullin et al., 2015; Tietze et al., 2015; Zhi et al., 2020). Various approaches have been explored to use SPIONs in cancer treatment strategies combined with other structures such as polymeric micelles, polysaccharides, polypeptides, carbon-based materials, or fluorescing molecules (Cryer and Thorley, 2019; Zhi et al., 2020). These strategies are mainly performed to improve SPIONs performance in biological environments in terms of biodistribution and biocompatibility (Vakili-Ghartavol et al., 2020; Zhi et al., 2020) and to reduce potential toxic effects caused by different types of SPION under certain conditions (Singh et al., 2010; Vakili-Ghartavol et al., 2020). The initial concentration is an important cause of these toxic effects. Even during the administration into the body, the SPION concentration may vary undesirably during transit through the tissues and body due to many factors. Some authors have reported that for concentrations above 200–500 $\mu\text{g/ml}$ (depending on the study), the toxic effect of conventional SPIONs increases (Naqvi et al., 2010; Singh et al., 2010; Dulińska-Litewka et al., 2019; Vakili-Ghartavol et al., 2020). Despite the fact that some studies have shown biocompatibility during the first 24 h and in concentrations below 100 $\mu\text{g/ml}$ (Rahimnia et al., 2019), for applications where higher density of magnetic particles is needed, the alternatives to reduce the cytotoxicity are still under discussion. Some of these approaches have been recently explored; one concept involves coating the SPIONs by

using different hydrophobic or hydrophilic materials such as polyethylene glycol (PEG), Polyvinyl Alcohol (PVA), lipids, and even cell membrane material (Bloemen et al., 2012; Parodi et al., 2013; Zaloga et al., 2014; Chen et al., 2017; Cryer and Thorley, 2019). Another approach is integrating the SPIONs into a biocompatible polymeric matrix to reduce possible side effects (Solar et al., 2015; Li et al., 2016; Idris et al., 2018). In concordance with these approaches, poly (3-hydroxybutyrate-co-3-hydroxyvalerate) (PHBV), a biodegradable polymer applied in the development of drug delivery capsules (Li et al., 2016; Idris et al., 2018), may be used to load surface-modified SPIONs to buffer the side effects of highly concentrated SPIONs in cells.

Curcumin is a phytotherapeutic compound with antioxidant properties and features, including wound healing effects and reduction of oxidative stress in cells (Gopinath et al., 2004; Pulido-Moran et al., 2016; Qi et al., 2020; Rahaman et al., 2020). In addition, it has shown good entrapment efficiencies and release rates through formulations using polyhydroxyalkanoates (PHA) (Senthilkumar et al., 2017; Mutlu et al., 2018; Aguilar-Rabiela et al., 2020; Aguilar-Rabiela et al., 2021). In this work, lauric acid-coated SPIONs (SPION^{LA}), which have been proven to be biocompatible in concentrations of around 200 $\mu\text{g/ml}$, were incorporated into PHBV-based microspheres at different and larger concentrations to develop magnetic microcapsules with curcumin releasing capability. Subsequently, the cell viability of the novel composite microcapsules during the first 7 days of

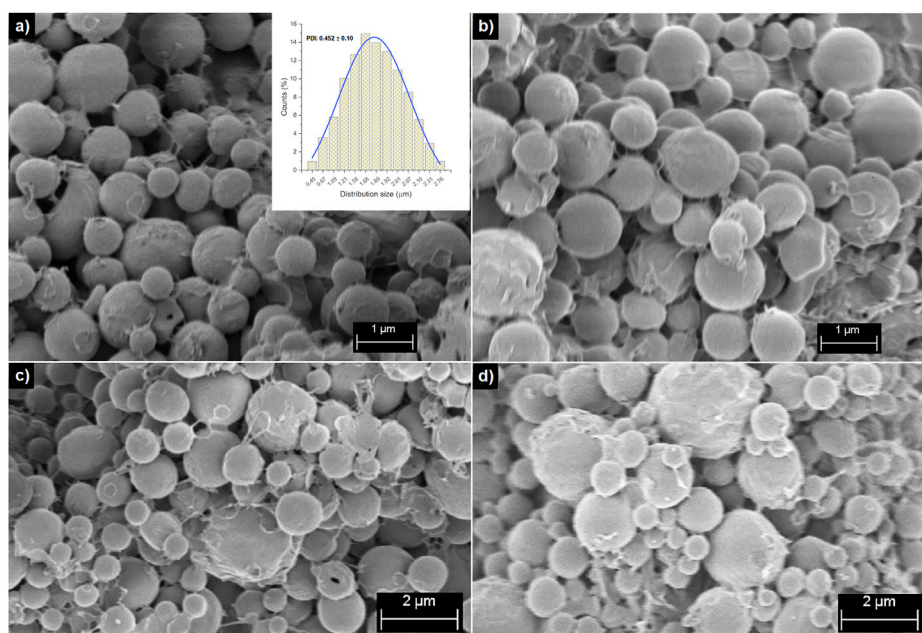


FIGURE 1

SEM micrographs of PHBV/SPION^{LA} composite at (A) 5:2, (B) 10:1 and (C) 10:3 ratios, and (D) PHBV microspheres without loading.

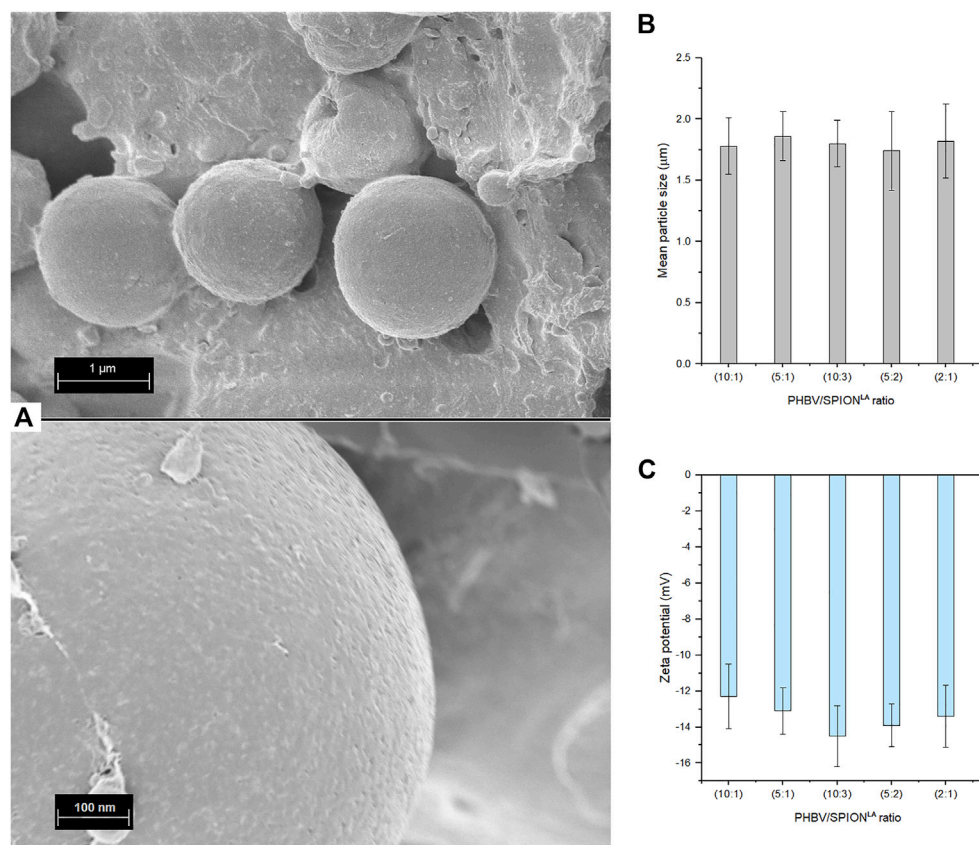


FIGURE 2

(A) SEM micrographs showing the surface morphology of PHBV/SPION^{LA} composite microspheres at 10:1 ratio, (B) mean particle size measured in PBS (pH:7.4) and (C) Zeta potential of PHBV/SPION^{LA} composite microspheres measured in deionized water. (SD as error bars, $n = 4$)

administration was determined and compared with that of pristine SPION^{LA}.

Results and DISCUSSION

Particle size, morphology, and zeta potential

Homogeneous and soft spherical-shaped (Figure 1) PHBV-based microspheres were fabricated. The composite microspheres exhibited a semi-smooth surface morphology with low porosity (Figure 2A). Apparently, the shape of the composite microspheres was not affected by the incorporation of SPION^{LA} and curcumin at the ratios studied in this work. Similar shape and morphology were observed for all the studied conditions and PHBV microspheres without loading. The homogeneous spherical shape and surface morphology should promote a uniform drug release by diffusion, in agreement with previous work on PHAs-based microspheres produced by

emulsion technique (Monnier et al., 2016; Nguyen and Jeong, 2018; Aguilar-Rabiela et al., 2020).

The average diameters of composite microspheres dispersed in deionized water are shown in Figure 2B. The size range of the composite microspheres and their homogeneity in shape are similar to those previously reported (Li et al., 2016; Monnier et al., 2016; Idris et al., 2018; Aguilar-Rabiela et al., 2021). The Zeta potential of composite microspheres is shown in Figure 2C. The values measured in this aqueous environment are moderately stable, suggesting that composite microspheres will not agglomerate quickly *in vivo* and *in vitro* applications, at least in conditions with similar pH, aqosity, and ion concentration (Hill et al., 1977; Kaewsichan et al., 2011). Besides, it is possible that microspheres, due to their size, tend to precipitate in static conditions and after a specific time. The Zeta potential values can be explained due to the hydrophobicity of PHBV and curcumin. However, similar Zeta potential values have been observed in previous works with PHBV-based particles used for drug release purposes (Francis et al., 2011; Masood et al., 2013).

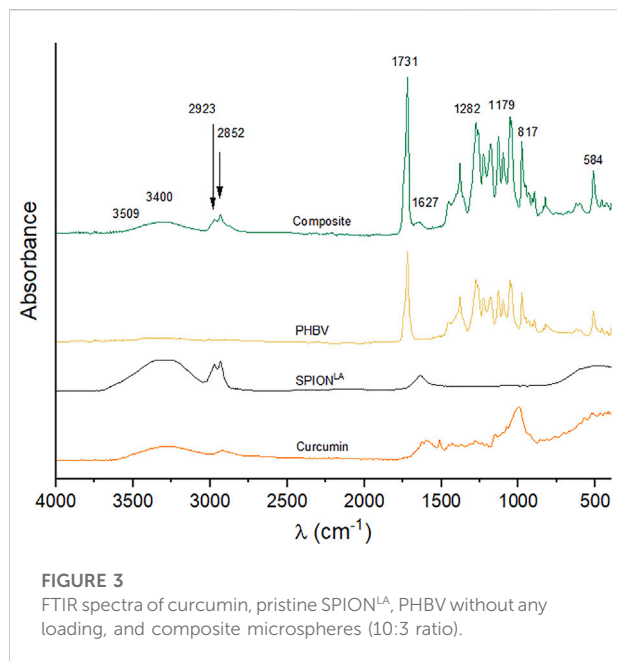


FIGURE 3
FTIR spectra of curcumin, pristine SPION^{LA}, PHBV without any loading, and composite microspheres (10:3 ratio).

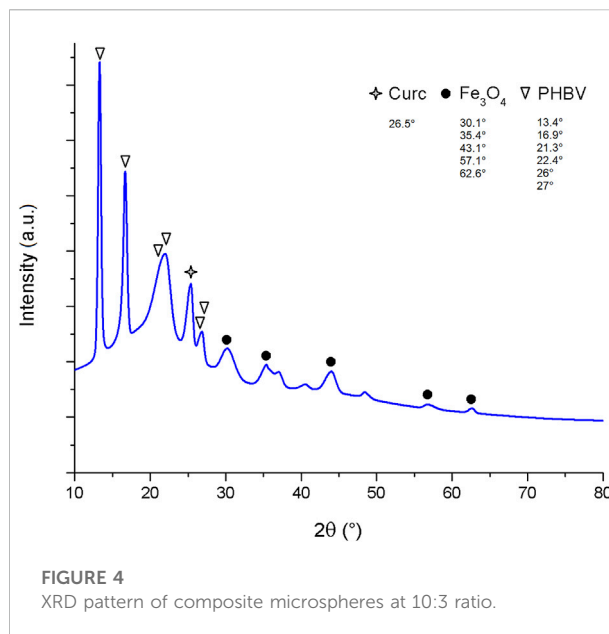


FIGURE 4
XRD pattern of composite microspheres at 10:3 ratio.

Composition analysis

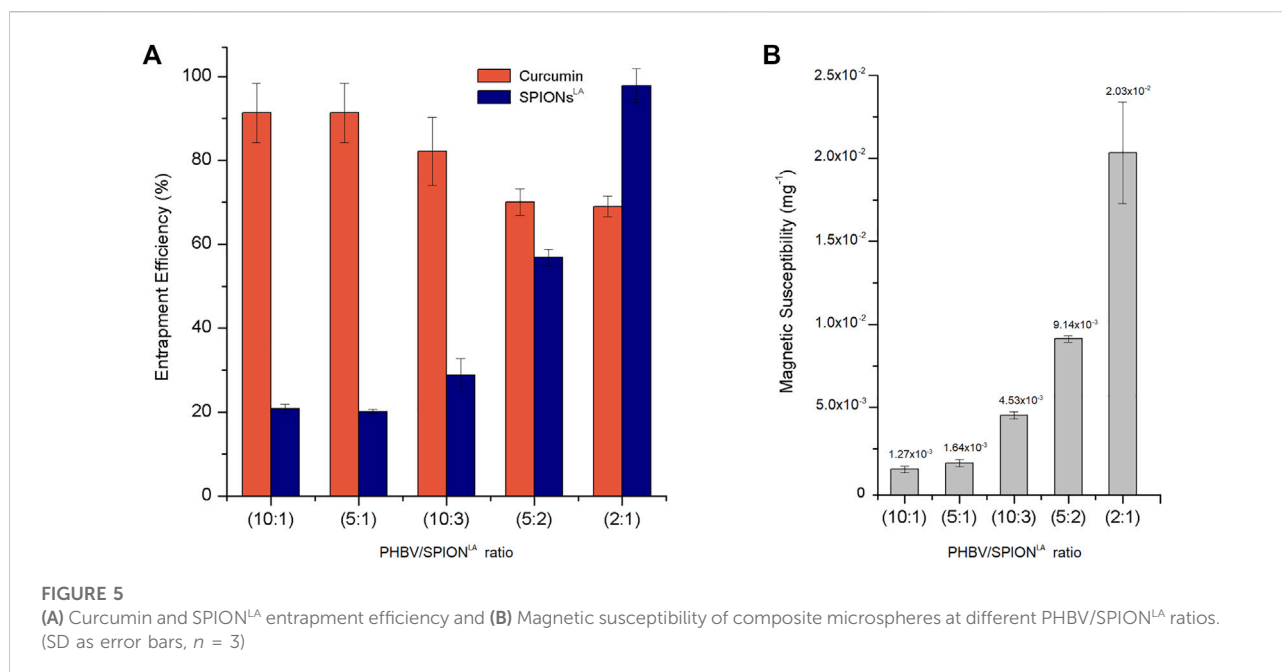
The FTIR spectra of curcumin, SPION^{LA}, blank PHBV microspheres, and composite microspheres are shown in [Figure 3](#). In the FTIR curve of composite microspheres, the spectrum of PHBV is observable with characteristic peaks at 1731 cm⁻¹, indicating the stretching mode of C = O in the crystalline phase ([Aguilar-Rabiela et al., 2021](#)). The peaks at 1,282 cm⁻¹ and 1,179 cm⁻¹ correspond to C–O–C stretching modes of the crystalline and amorphous parts, respectively ([Aguilar-Rabiela et al., 2021](#)). The spectrum of composite microspheres also exhibits the beginning of a band at 3,509 cm⁻¹ which reaches its maximum at about 3,400 cm⁻¹. These bands have been reported previously as the vibrations of -CH bonds and the stretching of hydrogen bonded -OH groups, respectively, of curcumin ([Athira and Jyothi, 2014](#); [Chidambaram and Krishnasamy, 2014](#); [Kazemi-Darabadi et al., 2019](#)). Another expected peak of curcumin at 817 cm⁻¹, corresponding to the O-H stretch, was probably overlapped under the intense peaks of PHBV. On the other hand, despite some characteristic peaks of the vibration of Fe–O from Fe₃O₄ at 584 cm⁻¹ ([Iyengar et al., 2014](#); [Li et al., 2016](#); [Idris et al., 2018](#)), which was probably overlapped by the intense spectrum of PHBV, it was still possible to observe the absorption bands at 2,852 cm⁻¹ and 2,923 cm⁻¹ corresponding to the symmetric and asymmetric C-H stretching from lauric acid also present in SPION^{LA} ([Si et al., 2013](#); [Idris et al., 2018](#)). Although these two groups were also present in curcumin, another characteristic peak near 1,627 cm⁻¹ is observed, which was previously reported due to the adsorption of water molecules to the surface of

SPIONs *via* hydrogen bond ([Sodipo et al., 2014](#); [Galli et al., 2017](#)). These results were complemented with the XRD analysis and the results of the release kinetic of curcumin to support the presence of the components in the composite microspheres.

The XRD diffractogram of composite microspheres is shown in [Figure 4](#). The characteristic peaks related to PHBV at 2θ 21.3° (101), 22.4° (111), 26° (130), and 27° (040) are clearly observed, and the intensity of the peaks at 13.4° (020), 16.9° (110) indicates the presence of orthorhombic unit cells in PHBV ([Li et al., 2016](#); [Idris et al., 2018](#); [Aguilar-Rabiela et al., 2021](#)). The peaks at 2θ 30.1° (220), 35.4° (311), 43.1° (422), 57.1° (511), and 62.6° (440) correspond to a cubic spinel structure present in SPION^{LA} ([Li et al., 2016](#); [Idris et al., 2018](#)). Finally, the peak at 2θ 26.5° may correspond to crystalline curcumin ([Van Nong et al., 2016](#)), however this could be also overlapped with the strong peak of PHBV at 26°.

Entrapment efficiency and magnetic susceptibility

[Figure 5A](#) shows the curcumin entrapment efficiency (CEE) and SPION^{LA} entrapment efficiency (SEE) measured in the composite microspheres at the studied ratios. As the concentration of SPION^{LA} increases, the SEE in the microspheres increases as well. On the other hand, the CEE decreases while increasing the SEE. This behavior is possibly due to the integration of lauric acid present on SPION^{LA}, which modifies the hydrophobicity of the emulsion and thus



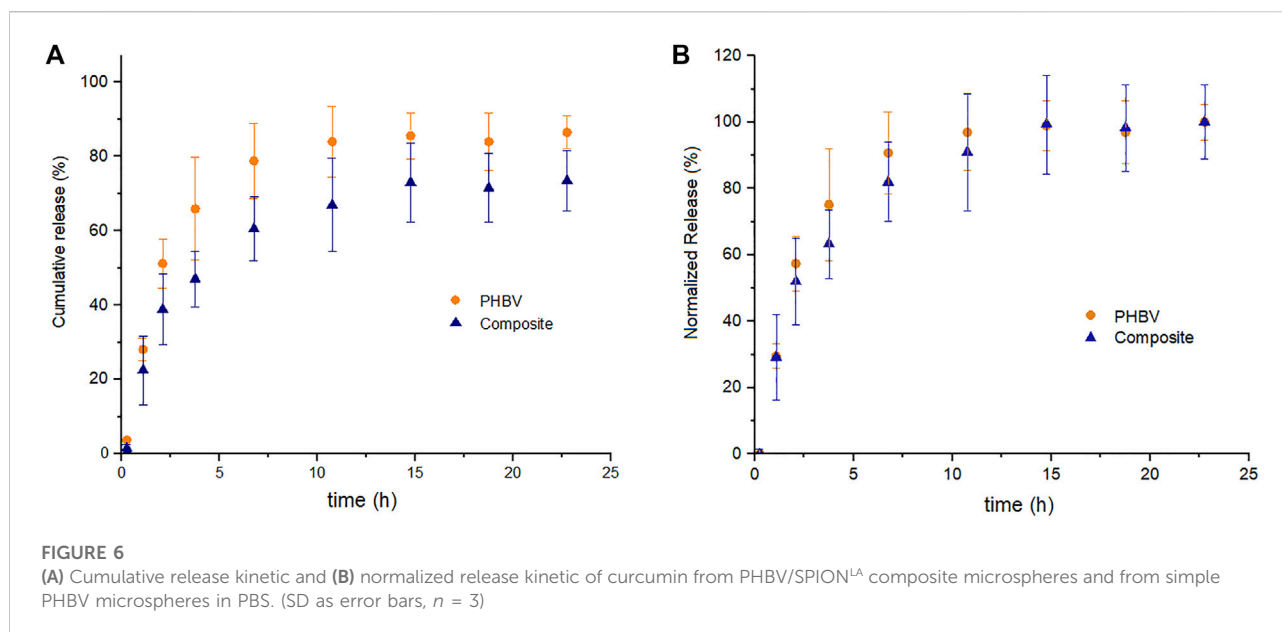
may hamper the interaction between PHBV, curcumin, and the used organic solvent, leading to reduced incorporation of curcumin (Ghalandarlaki et al., 2014; Law, 2014; Zhan et al., 2020). Nevertheless, the CEE was above 80% for the 10:1, 5:1, and 10:3 ratios, and over 60% for the 5:2 and 2:1 ratios; this means a CEE above 60% for all the conditions studied which is better compared to the entrapment efficiency exhibited during the loading of other substances such as antibiotics (Francis et al., 2011). As reported before, the hydrophobicity and chemical structure of the drug to entrap impact the entrapment efficiency of PHA matrices (Francis et al., 2011; Grillo et al., 2011; Heathman et al., 2014). The CEE results showed the potential of all composite formulations for the loading of curcumin which may be extended to similar phytotherapeutics (Abd El-Hay et al., 2016; Aguilar-Rabiela et al., 2020).

The apparent inverse relationship between CEE and SEE may modify the magnetic susceptibility of the composite along the ratios studied as less iron amount is contained in the polymer matrix. The magnetic susceptibility of 1 mg of composite microsphere samples from each condition is shown in Figure 5B. As expected, the magnetic susceptibility value increases in correspondence with the SEE of each sample. However, the magnetic susceptibility measured for all the composite conditions is between $\times 1210^{-4} \text{ mg}^{-1}$ and 0.02 mg^{-1} , which means the microspheres can be influenced by magnetic forces in direct correlation to the SPION loading ratio of the sample. Besides, some of these magnetic susceptibility values are similar to those in previous studies which have used PHA matrix formulations (Idris et al., 2018).

Release kinetics

The release kinetic of curcumin from composite microspheres at the highest SPION^{LA} concentration (2:1) and PHBV microspheres without SPION^{LA} (both at 10:1 curcumin ratio) was compared (Figure 6). The total cumulative release of curcumin from the composite microspheres seemed to be lower than the cumulative release from PHBV microspheres (Figure 6A); this apparent difference is explained due the CEE behavior discussed in the previous section, where the CEE decreases with the incorporation of SPION^{LA} in comparison with the CEE observed in conventional PHBV microspheres (around 90%) and also corresponding with the entrapment efficiency values previously reported (Aguilar-Rabiela et al., 2020; Aguilar-Rabiela et al., 2021). However, the normalized release with respect to the total release was quite similar (Figure 6B); this means that the incorporation of SPION^{LA} into the PHBV matrix did not modify the curcumin release behavior of the composite at least in the ratios studied. Besides, both release kinetics exhibit the typical initial “burst release phase”, within the first 4 h, followed by a delayed release, also called the “controlled release phase”, from 4 to 15 h until stabilization. This release behavior was in concordance with previous release kinetics observed in PHA-based microsphere formulations (Monnier et al., 2016; Aguilar-Rabiela et al., 2020; Aguilar-Rabiela et al., 2021).

The release behavior observed in the composite may allow gradual release of certain phytotherapeutics such as curcumin and possibly be applied in developing prolonged treatments with less periodical administration. This gradual release can also



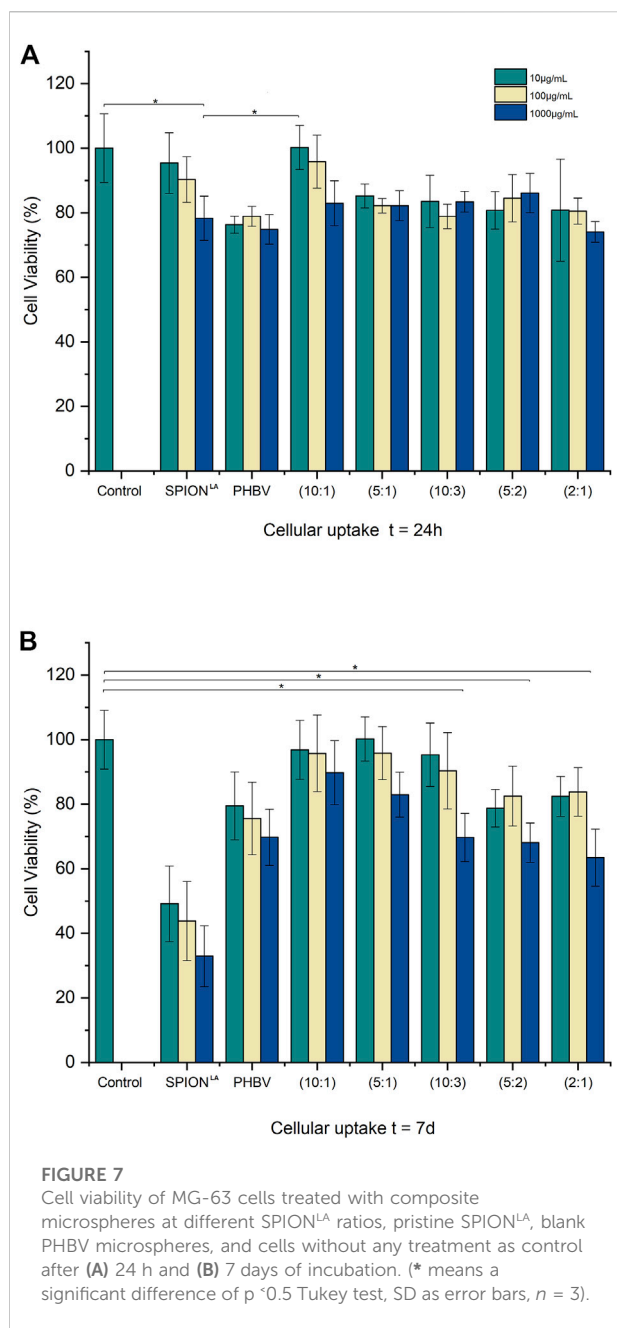
prevent sudden high concentrations of drugs during the early administration stages, in contrast to conventional drug delivery devices, which once dissolved, release the complete concentration in the media (Mehrotra et al., 2007; Liechty et al., 2010). Additionally, this release behavior may be helpful in applications that require a time window for positioning the microspheres in specific tissues or organs before starting the release. Composites such as the studied could bring the time to magnetically target the particles into particular zones and to localize the drug delivery. The biodegradable PHBV matrix also brings a period of time before releasing any additional materials incorporated into the composite (such as the SPION^{LA}) to the biological environment, which may help reduce the possible side effects due to an undesirable accumulation of these nanoparticles. As has been observed in previous works, PHA based particles can be tunable by blending with other materials or by copolymerization, among other techniques, to modify the release rate of the components and substances loaded into the resultant matrix and, in some cases, changing also the biodegradation rate, which may help to damp the possible side effects of a burst release of the incorporated components (Grillo et al., 2011; Panith et al., 2016; Pérez-Arauz et al., 2019; Aguilar-Rabiela et al., 2021).

Cytocompatibility of composite microspheres

The cell viability of each condition of PHBV/SPION^{LA}/curcumin composite microspheres, PHBV microspheres without any loading, pristine SPION^{LA}, and cells without any treatment as control, were measured and compared after two different time sets of incubation (Figure 7). WST-8 assay was

used to correlate the cell viability of all conditions, as used in several previous works (Filipova et al., 2018; Idris et al., 2018; Aguilar-Rabiela et al., 2020; Aguilar-Rabiela et al., 2021). Viability measurements were taken after 24 h and after 7 days of incubation on cell cultures treated with similar calculated amounts of SPION^{LA} administrated through the different composite ratios and compared to an equivalent quantity of pristine SPION^{LA}. After the first 24 h of incubation, most conditions exhibited similar cell viability values to the control (Figure 7A), except for the blank PHBV microspheres, which showed lower viability values. This behavior may be explained due to an elevated amount of PHBV that could impact the cell viability during incubation, which is in agreement with similar behavior observed in previous publications, which showed that a large amount of PHBV may reduce cell viability (Balakrishna Pillai et al., 2020; Aguilar-Rabiela et al., 2021). In contrast, all composite microspheres conditions exhibited cell viability values comparable to the control, being the 10:1 ratio the condition exhibiting the highest cell viability values. This behavior can be attributed to the release of curcumin and its antioxidant properties which, combined with the controlled release of SPIONs^{LA} to the medium, reduces the side effects. Similar beneficial effects in cell culture have been observed in previous investigations (Ghalandarlaki et al., 2014; Qi et al., 2020; Aguilar-Rabiela et al., 2021).

After 7 days of incubation, a reduction in cell viability in the samples treated with pristine SPION^{LA} was observed compared to the control (Figure 7B). Similar behavior was observed in blank PHBV microspheres. In contrast, most samples treated with composite microspheres still exhibited similar cell viability values to the control; even at the higher concentrations, the cell viability values were over 60% compared to the control.



Apparently, as the SPION^{LA} ratio decreases, the cell viability increases; this trend was observed in the three dilutions used in the present experiments. This behavior suggests that the biocompatibility of similar amounts of SPION^{LA} improved through its administration by the composite microspheres instead of free administration. Many factors may be involved in this behavior; one of them is the size interaction between cells and particles, which has been reported previously to impact cell viability *in vitro* (Wei et al., 2014).

In the case of samples treated with pristine SPION^{LA}, the total concentration of the nanoparticles is likely in direct contact with

the cell membrane since the beginning of the administration, which is not the case for the contact interaction between composite microspheres and cells, due to the larger size of the microspheres. Besides, during the beginning of the composite administration, a large portion of SPION^{LA} is expected to be still entrapped in the composite particles, which results in an effective interaction only between cells and PHBV microparticles, mainly by contact or adhesion. On the other hand, with pristine SPION^{LA} administration, undesirable accumulation may occur resulting in a different interaction with the cell membrane due to the size of the nanoparticles. Then, the composite may allow the gradual release of SPION^{LA} into the biological medium; this can maintain lower concentrations of nanoparticles in contact with the cells leading, under this condition, to biocompatible behaviour (Zaloga et al., 2014; Idris et al., 2018). This gradual release may also improve the mineralization of the iron-based nanoparticles. Although the present results cannot characterize the release kinetics of the SPION^{LA} into the biological medium, the cell viability behavior can be compared with those previously observed when other nanoparticles were incorporated into PHA matrices (Aguilar-Rabiela et al., 2021). The prolonged release of curcumin may also reduce the side effects by decreasing the cell stress during the mineralization process; as reported before, curcumin helps reduce the oxidative stress of cells during incubation (Mahmoudi et al., 2010; Ghalandarlaki et al., 2014; Patil et al., 2018; Zhi et al., 2020; Aguilar-Rabiela et al., 2021). The slightly decreasing cell viability on the samples treated with blank PHBV microspheres is also in concordance with the beneficial effect of curcumin in samples treated with the composite.

In addition, fluorescent microscopy images were taken to observe the morphology of cells treated with composite microspheres at 10:1, 10:3, and 2:1 ratios and with proportional concentrations of pristine SPION^{LA}, respectively. Cell's nuclei (green) and cytoplasm (red) were stained for observation, and the bright field was overlapped to observe the distribution of the different particles (white). Fluorescent micrographs taken after 24 h were compared to observe differences in cell morphology (Figures 8A,B). After 24 h of incubation, both samples exhibited the typical morphology of healthy MG-63 cells, colonies with defined nuclei conformed by homogeneous and well-spread cytoplasm. This observation is in agreement with respective WST-8 viability results.

However, after 7 days of incubation, the fluorescent micrographs of cells treated with pristine SPION^{LA} exhibited anomalies in the cell morphology with a less spread cytoplasm and heterogeneous shaped cytoplasm (Figure 8C). This is in contrast to samples treated with composite microspheres at 10:3, which still showed homogeneously conformed cell colonies, some cells apparently adhered around the microspheres and with well-defined cytoplasm (Figure 8D). Both observations corresponded with the respective cell viability result. Additionally, samples treated with composite microspheres at the highest ratio (2:1) were compared with a similar amount of

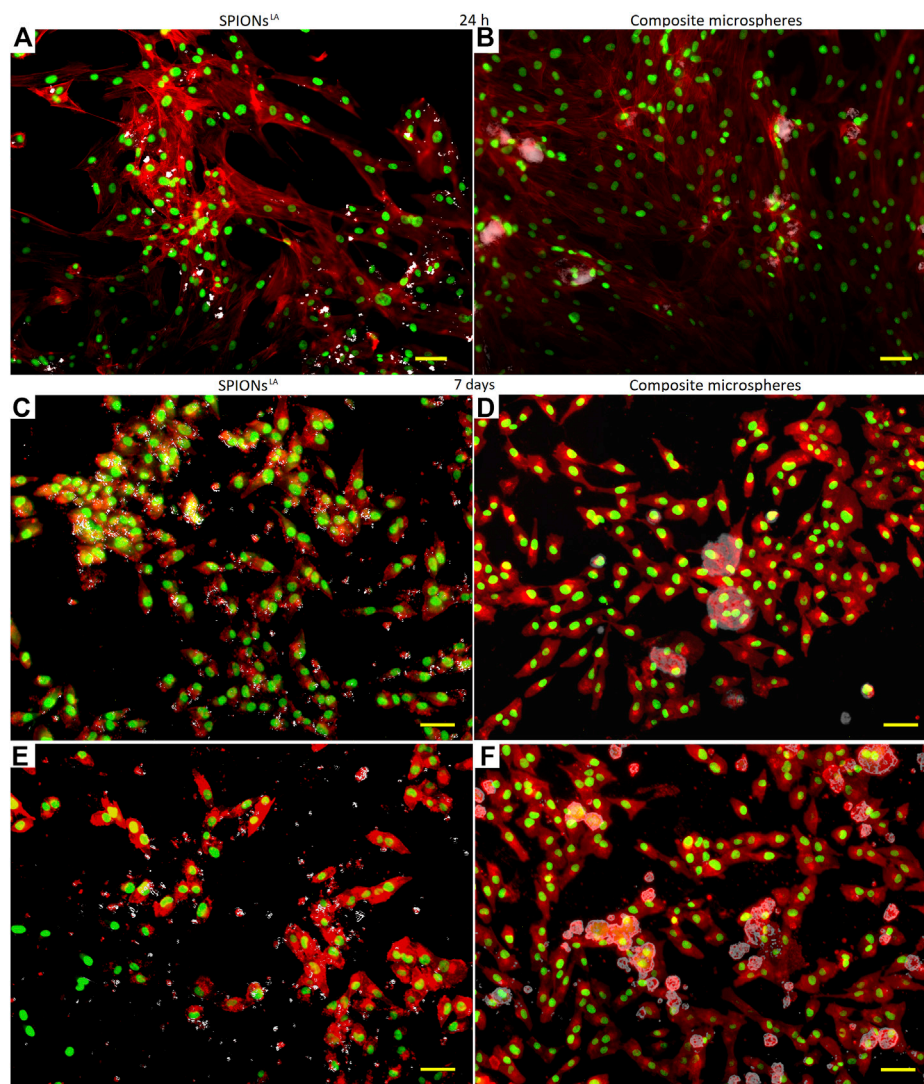


FIGURE 8

Fluorescence microscopy images of (A) pristine SPION^{LA}, (B) composite microspheres at 10:1 ratio after 24 h of incubation, (C) pristine SPION^{LA}, (D) composite microsphere at 10:3 ratio, (E) pristine SPION^{LA}, and (F) composite microsphere at 2:1 ratio, after 7 days of incubation with MG-63 cells. (bar size is 2 μm).

pristine SPION^{LA}. In the sample treated with pristine SPION^{LA} (Figure 8E), it is possible to observe some agglomeration of pristine SPION^{LA} among cells and a reduction of the cell population; the cytoplasm morphology may be explained due to a low cell-matrix attachment; even some nuclei and cytoplasm looked dispersed, possibly due to a membrane rupture as it has been previously reported (Mahmoudi et al., 2010).

In contrast, a larger group of healthy cells (homogeneous colonies of semi-spread cells with well-formed cytoplasm) was observed after 7 days of the composite administration (Figure 8F). Some microspheres can be observed, some of them are surrounded by cells similar to Figure 8D, and no pristine SPION^{LA} agglomerations appeared. This supported

the idea that most SPION^{LA} remained in the PHBV matrix during this period. Furthermore, in all the observations on samples treated with composite microspheres, the cells appeared to be attached around the microspheres (Figures 8B,D,F), supporting the interaction between composite microspheres and cells by adhesion. The correspondence of the observations to WST-8 cell viability results confirms a significantly different behavior between both SPION^{LA} administration modes.

The favorable fluorescent microscopy observations and cell viability results can be attributed to the beneficial effect of the prolonged release of curcumin during incubation (Gopinath et al., 2004; Qi et al., 2020; Rahaman et al., 2020; Aguilar-

Rabiela et al., 2021). Qualitative and quantitative results show favorable biocompatibility upon the administration of large concentrations (above 500 $\mu\text{g/ml}$) of SPION^{LA} after 7 days of incubation. This result confirms the composite potential for applications in which higher magnetic susceptibility properties are required. Besides, the prolonged release of an antioxidant agent to reduce cell stress (Wei et al., 2012; Wei et al., 2014; Aguilar-Rabiela et al., 2021), and the possible controlled release of SPION to the biological medium suggest the use of this PHBV/curcumin composite as an adequate interface for damping the toxicity that can occur upon administering other SPION formulations.

Conclusion and outlook

PHBV/SPION^{LA}/curcumin composite microspheres developed in this study exhibited an effective curcumin entrapment efficiency with no significant interference due to the incorporation of SPION^{LA} at the ratios studied. The *in vitro* cell viability results and cell morphology observations showed a significant difference in the behavior of MG-63 cells, after 7 days of incubation, due to exposure to a similar concentration of pristine SPION^{LA} compared to its administration through the composite microspheres. These results, supported quantitatively by WST-8 cell viability assay and qualitatively by fluorescent microscopy observations, suggest that the combination of the PHBV matrix and the prolonged release of curcumin may reduce the possible side effects of the administration of high concentrations of SPION^{LA} applied *in vitro*. Besides, the curcumin release kinetics observed may provide a time window for the magnetic positioning of the composite microspheres in specific organs or tissues before the release. The approach could be helpful for the release of similar substances for targeted delivery treatments which require a larger density of magnetic particles than studied previously. Although more studies are needed to characterize the mechanism of SPION^{LA} release from the PHBV matrix and to analyze the SPION^{LA} concentration in the biological environment along the time, the results presented show that this composite technology may be suitable for the administration of different SPION formulations with reduced possible toxic effects. Additional research on this approach will add knowledge and contribute to the development of SPION based localized drug delivery platforms.

Materials and methods

Materials

PHBV was purchased from Goodfellow (Bad Nauheim, Germany), dichloromethane (DCM), lauric acid (LA) and acetone from Sigma-Aldrich (St. Louis, MO, United States), curcumin from Sigma-Aldrich (Steinheim, Germany), and

Polyvinyl Alcohol (PVA) from Baxter Healthcare (Opfikon, Switzerland). Iron (II) chloride tetrahydrate ($\text{FeCl}_2 \cdot 4\text{H}_2\text{O}$), hydroxylammonium chloride and bovine serum albumin (BSA) were obtained from Merck (Darmstadt, Germany). Iron (III) chloride hexahydrate ($\text{FeCl}_3 \cdot 6\text{H}_2\text{O}$), dialysis tubes (Spectrapor6, MWCO 8 kDa), ammonium chloride, hydrochloric acid (25%), and ammonia solution 25% were supplied by Roth (Karlsruhe, Germany). The Lauric acid-coated SPIONs (SPION^{LA}) were provided and characterized by the Section of Experimental Oncology and Nanomedicine (SEON) of *HNO-Klinik* (Erlangen, Germany), they were synthesized according to the protocol reported previously (Zaloga et al., 2014). Briefly, FeCl_2 , and FeCl_3 were mixed in water and heated to 90°C while stirring under an argon atmosphere. After adding ammonia, lauric acid, dissolved in acetone, was added to the prepared blackish dispersion. After further stirring at 90°C, the particles were cooled to room temperature and purified *via* dialysis. The formed SPION^{LA} stock solution was stored at 4°C until microsphere fabrication. All chemicals used were of analytical grade.

Composite microspheres fabrication

Composite PHBV-SPION^{LA}-curcumin microspheres were fabricated using a modified solid-in-oil-in-water (S/O/W) emulsion-solvent evaporation method as previously reported (Idris et al., 2018; Aguilar-Rabiela et al., 2021). Different amounts of the SPIONs^{LA} stock solution were added to 10 ml of PHBV-DCM solution to prepare the five conditions: from 10% to 50% of SPION^{LA} (w/w), respectively 10:1, 5:1, 10:3, 5:2, 2:1 PHBV/SPIONs^{LA} mass ratios. Posteriorly, curcumin was added for all the conditions at a constant mass ratio of 10:1 (PHBV/curcumin). Then the resulting solution was mixed at 800 rpm with a mechanical mixer to conform to the S/O phase. Simultaneously, an aqueous solution of 1 mg/ml of PVA was prepared and mixed at 600 rpm to form the W phase, and later both phases were mixed at 19,000 rpm using a homogenizer T18 (IKA, Staufen, Germany). Afterward, the emulsion was centrifuged at 6,000 rpm in a 5804 R (Eppendorf, Germany) and washed two times with ultrapure water, and the supernatant was removed entirely. Subsequently, the precipitated microspheres were dried overnight in an incubator at 60°C and later stored protected from the light.

Curcumin entrapment efficiency

The Curcumin Entrapment Efficiency (CEE) was determined according to a modified supernatant method previously reported (Zidan et al., 2011; Aguilar-Rabiela et al., 2020). Briefly, composite microspheres were immersed in ethanol; after depletion, the curcumin concentration in the supernatant was measured using a UV/Vis spectrophotometer Specord 250 (Analytikjena, Jena,

Germany) at 425 nm (Senthilkumar et al., 2017). The entrapment efficiencies were calculated by using the initially added curcumin amounts during the fabrication, the curcumin measured by concentration, and the following equation (Aguilar-Rabiela et al., 2020; Aguilar-Rabiela et al., 2021):

$$CEE = \frac{(M_{the} - M_{sup}) \cdot 100\%}{M_{the}} \quad (1)$$

where M_{sup} is the curcumin in the supernatant in mg, and M_{the} is the initial mass of curcumin added during the fabrication of the microspheres in mg.

Magnetic susceptibility and SPION^{LA} entrapment efficiency

For the magnetic susceptibility measurements, 1 mg of dried microspheres were placed in a measuring tube of a single frequency (1 kHz) magnetic volume susceptibility measuring device MS2G (Barrington, Witney, United Kingdom).

The SPION^{LA} entrapment efficiency (SEE) was calculated by correlating the iron content measured on microsphere samples, the iron content in the pristine SPION^{LA} (previously measured) added during the fabrication of each composite condition, and the following equation (Li et al., 2016):

$$SEE = \frac{I_{mea} \cdot 100\%}{I_{the}} \quad (2)$$

where I_{mea} is the iron mass amount measured in the microspheres in μg and I_{the} is the initial iron mass amount (calculated from the initial mass amount in SPION^{LA}) added in μg .

The iron content of composite microspheres and SPION^{LA} was measured at SEON (*HNO-Klinik*, Erlangen, Germany), similar to previous reports (Idris et al., 2018). Briefly, samples were dispersed in 100 μL of 65% nitric acid (HNO_3) solution and cooked at 95°C for 15 min. Then 500 μL of HNO_3 were added, and 20 μL were taken from the resulting solution and mixed with 1980 μL of water in triplicate for the measurements by microwave plasma atomic emission spectroscopy using a 4200 MP-AES (Agilent, CA, United States).

Particle size and zeta potential analysis

The particle size average and zeta potential measurements of each condition of the composite microspheres and blank PHBV particles were carried by using a Zetasizer Nano ZS (Malvern, Worcestershire, United Kingdom) in PBS (pH: 7.4) and deionized water, considering a working concentration of 0.1 mg/ml per sample, similarly to previous reports (Zaloga et al., 2014; Idris et al., 2018; Aguilar-Rabiela et al., 2021).

Surface morphology of composite microspheres

The surface morphology of the PHBV-SPION^{LA}-curcumin microspheres was observed by Scanning Electron Microscopy (SEM) (FE-Auriga, Carl-Zeiss, Munich, Germany). The composite microsphere samples were sputtered with gold in a turbomolecular pumped coater Q150T Plus (Quorum, Laughton, United Kingdom) prior to SEM examination at 1.9 kV of acceleration voltage and using secondary electrons detector.

Structural characterization of composite microspheres

The structural characterization of the composite microspheres was determined through FTIR by using a Nicolet 6,700 Thermo Scientific FTIR spectrometer (Waltham, MA, United States). Measurements were carried out in absorbance mode at wavenumber range from 4,000 to 400 cm^{-1} at a resolution of 4 cm^{-1} . X-ray diffraction (XRD) analysis was performed using an X-ray diffractometer Miniflex 600 (Rigaku, Tokyo, Japan) in the 2θ range of 10°–80° with a step size of 0.01° and dwell time of 1/min.

Curcumin release kinetics

To determine the curcumin release kinetics, 10 mg of composite microspheres at 2:1 ratio and PHBV microspheres loaded with curcumin at the same ratio were previously rinsed with ethanol to remove the excess curcumin in the supernatant and with water to remove any remanent solvent. Once dried, microsphere samples were placed in sterile falcon tubes with caps in triplicate. Then 10 ml of phosphate buffer solution (PBS) at pH 7.4 (Sigma-Aldrich, Steinheim, Germany) was added to each falcon tube which were then stored at room temperature, protected from light according to previous works (Aguilar-Rabiela et al., 2020; Aguilar-Rabiela et al., 2021). The release kinetic curve was obtained photospectroscopically using a Specord 250 device (Analytik Jena, Jena, Germany) at 425 nm, similarly to previously reported (Zidan et al., 2011; Aguilar-Rabiela et al., 2020; Aguilar-Rabiela et al., 2021).

Cytocompatibility assays

MG-63 human osteoblast-like cells (Sigma-Aldrich, Germany) were grown in Dulbecco's Modified Eagle Medium (DMEM) supplemented with 10% FBS (Gibco, Dreieich, Germany). After a confluence of approx. 80%, 50·10³ cells were seeded in 24 well-plates and incubated for 12 h before running the cytocompatibility assays.

The previously measured iron content in SPION^{LA} was used to calculate a solution of pristine SPION^{LA} containing 1 mg of iron per milliliter. Similarly, suspensions from each composite microsphere condition were calculated and prepared in order to have the same iron content (1 mg/ml). Afterward, ten-fold serial dilutions of 10 μ L, 100 μ L, and 1,000 μ L from each suspension were added to the 24 well-plates previously incubated with cells. A similar mass amount of blank PHBV microspheres was used as an additional condition, and cells without any treatment were used as control. All experiments were carried out in triplicate. The cell viability was determined by WST-8 assay (Sigma-Aldrich, Steinheim, Germany) after 24 h and 7 days post-treatment. Briefly, the supernatant was carefully removed from all well-plates and washed with PBS; later freshly prepared cell culture medium containing 1.0% *v/v* WST-8 solution was added to the 24 well-plates and incubated for 2 h. After incubation, 100 μ L of supernatant from each well-plate was transferred into a 96 well-plate for the absorbance measurement at 450 nm in a PHOmo Autobio (Labtec Instruments, Zhengzhou, China) similar to previous reports (Li et al., 2016; Idris et al., 2018; Aguilar-Rabiela et al., 2021).

Cell staining and imaging

Cell samples were treated with Fluorescent DNA stain (DAPI) and Vybrant DyeCycle staining (both reagents from Merck, Darmstadt, Germany) for cell morphology observation after 24 h and after 7 days of incubation. Fluorescent micrographs were obtained and processed using a microscope AxioCam ERc 5s Primovert (Zeiss, Munich, Germany). Nuclei were green-colored for better visual analysis.

Statistical analysis

Experiments were performed in triplicate. The standard deviation was expressed as error bars. The analysis for statistical significance for the cell biology results was conducted by analysis of variance One-Way ANOVA followed by Tukey test ($p < 0.05$), using the software Origin 8 (OriginLab, Northampton, MA, United States),

References

- Abd El-Hay, A. M., Naser, A., Badawi, A., Abd El-Ghaffar, M., Abd El-Wahab, H., and Helal, D. A. (2016). Biodegradable polymeric microcapsules for sustained release of riboflavin. *Int. J. Biol. Macromol.* 92, 708–714. doi:10.1016/j.ijbiomac.2016.07.076
- Aguilar-Rabiela, A. E., Hernández-Cooper, E. M., Otero, J. A., and Vergara-Porras, B. (2020). Modeling the release of curcumin from microparticles of poly(hydroxybutyrate) [PHB]. *Int. J. Biol. Macromol.* 144, 47–52. doi:10.1016/j.ijbiomac.2019.11.242

and data is presented as the mean \pm standard deviation of each measurement.

Data availability statement

The raw data supporting the conclusion of this article will be made available by the authors, without undue reservation.

Author contributions

Conceptualization, AA-R; data curation, AB; Formal analysis, AA-R and AB; investigation, AA-R; methodology, AA-R and AB; resources, AB and HU; supervision, AB; validation, HU and AB; writing—original draft, AA-R; writing—review and editing, HU, CA, and AB. All authors contributed to manuscript revision, read, and approved the submitted version.

Acknowledgments

We acknowledge Alina Grünewald (Institute of Biomaterials, University of Erlangen-Nuremberg) for technical support, and Consejo Nacional de Ciencia y Tecnología (CONACyT) and Deutscher Akademischer Austauschdienst (DAAD) for funding (Ref. 57552340).

Conflict of interest

The authors declare that the research was conducted in the absence of any commercial or financial relationships that could be construed as a potential conflict of interest.

Publisher's note

All claims expressed in this article are solely those of the authors and do not necessarily represent those of their affiliated organizations, or those of the publisher, the editors and the reviewers. Any product that may be evaluated in this article, or claim that may be made by its manufacturer, is not guaranteed or endorsed by the publisher.

- Aguilar-Rabiela, A. E., Leal-Egaña, A., Nawaz, Q., and Boccaccini, A. R. (2021). Integration of mesoporous bioactive glass nanoparticles and curcumin into PHBV microspheres as biocompatible composite for drug delivery applications. *Molecules* 26, 3177. doi:10.3390/molecules26113177

- Athira, G. K., and Jyothi, A. N. (2014). Preparation and characterization of curcumin loaded cassava starch nanoparticles with improved cellular absorption. *Int. J. Pharm. Pharm. Sci.* 6, 171–176.

- Balakrishna Pillai, A., Jaya Kumar, A., and Kumarapillai, H. (2020). Biosynthesis of poly(3-hydroxybutyrate-co-3-hydroxyvalerate) (PHBV) in *Bacillus aryabhattai* and cytotoxicity evaluation of PHBV/poly(ethylene glycol) blends. *3 Biotech.* 10(10), 32–10. doi:10.1007/s13205-019-2017-9
- Bloemen, M., Brullot, W., Gils, A., Luong, T. T., Verbiest, T., Geukens, N., et al. (2012). Improved functionalization of oleic acid-coated iron oxide nanoparticles for biomedical applications. *J. Nanoparticle Res.* 14 1100. doi:10.1007/s11051-012-1100-5
- Chen, H.-L., Hsu, F. T., Kao, Y. C. J., Liu, H. S., Huang, W. Z., Lu, C. F., et al. (2017). Identification of epidermal growth factor receptor-positive glioblastoma using lipid-encapsulated targeted superparamagnetic iron oxide nanoparticles *in vitro*. *J. Nanobiotechnology* 15 86–13. doi:10.1186/s12951-017-0313-2
- Chidambaram, M., and Krishnasamy, K. (2014). Nanoparticulate drug delivery system to overcome the limitations of conventional curcumin in the treatment of various cancers: A review. *Drug Deliv. Lett.* 4, 116–127. doi:10.2174/2210303103999131211110708
- Chomoucka, J., Drbohlavova, J., Huska, D., Adam, V., Kizek, R., and Hubalek, J. (2010). Magnetic nanoparticles and targeted drug delivering. *Pharmacol. Res.* 62, 144–149. doi:10.1016/j.phrs.2010.01.014
- Cryer, A. M., and Thorley, A. J. (2019). Nanotechnology in the diagnosis and treatment of lung cancer. *Pharmacol. Ther.* 198, 189–205. doi:10.1016/j.pharmthera.2019.02.010
- Dulińska-Litewka, J., Lazarczyk, A., Halubiec, P., Szafranski, O., Karnas, K., and Karewicz, A. (2019). Superparamagnetic iron oxide nanoparticles—current and prospective medical applications. *Materials* 12, 617. doi:10.3390/ma12040617
- Filipova, M., Elhelu, O. K., De Paoli, S. H., Fremuntova, Z., Mosko, T., Cmarko, D., et al. (2018). An effective 'three-in-one' screening assay for testing drug and nanoparticle toxicity in human endothelial cells. *PLoS One* 13, e0206557. doi:10.1371/journal.pone.0206557
- Francis, L., Meng, D., Knowles, J., Keshavarz, T., Boccaccini, A., and Roy, I. (2011). Controlled delivery of gentamicin using poly(3-hydroxybutyrate) microspheres. *Int. J. Mol. Sci.* 12, 4294–4314. doi:10.3390/ijms12074294
- Galli, M., Guerrini, A., Cauteruccio, S., Thakare, P., Dova, D., Orsini, F., et al. (2017). Superparamagnetic iron oxide nanoparticles functionalized by peptide nucleic acids. *RSC Adv.* 7, 15500–15512. doi:10.1039/c7ra00519a
- Ghalandarlaki, N., Alizadeh, A. M., and Ashkani-Esfahani, S. (2014). Nanotechnology-applied curcumin for different diseases therapy. *Biomed. Res. Int.* 2014, 394264. doi:10.1155/2014/394264
- Gopinath, D., Ahmed, M., Gomathi, K., Chitra, K., Sehgal, P., and Jayakumar, R. (2004). Dermal wound healing processes with curcumin incorporated collagen films. *Biomaterials* 25, 1911–1917. doi:10.1016/s0142-9612(03)00625-2
- Grillo, R., Pereira, A. d. E. S., de Melo, N. F. S., Porto, R. M., Feitosa, L. O., Tonello, P. S., et al. (2011). Controlled release system for ametryn using polymer microspheres: Preparation, characterization and release kinetics in water. *J. Hazard. Mat.* 186, 1645–1651. doi:10.1016/j.jhazmat.2010.12.044
- Heathman, T. R. J., Webb, W. R., Han, J., Dan, Z., Chen, G. Q., Forsyth, N. R., et al. (2014). Controlled production of poly(3-hydroxybutyrate-co-3-hydroxyhexanoate) (PHBHx) nanoparticles for targeted and sustained drug delivery. *J. Pharm. Sci.* 103, 2498–2508. doi:10.1002/jps.24035
- Hill, E. P., Power, G. G., and Gilbert, R. D. (1977). Rate of pH changes in blood plasma *in vitro* and *in vivo*. *J. Appl. Physiol. Respir. Environ. Exerc. Physiol.* 42, 928–934. doi:10.1152/jappl.1977.42.6.928
- Idris, M. I., Zaloga, J., Detsch, R., Roether, J. A., Unterweger, H., Alexiou, C., et al. (2018). Surface modification of SPIONs in PHBV microspheres for biomedical applications. *Sci. Rep.* 8, 7286–7311. doi:10.1038/s41598-018-25243-9
- Iyengar, S. J., Joy, M., Ghosh, C. K., Dey, S., Kotnala, R. K., and Ghosh, S. (2014). Magnetic, X-ray and Mössbauer studies on magnetite/maghemite core-shell nanostructures fabricated through an aqueous route. *RSC Adv.* 4, 64919–64929. doi:10.1039/c4ra11283k
- Kaewsichan, L., Riyapan, D., Prommajan, P., and Kaewsrichan, J. (2011). Effects of sintering temperatures on micro-morphology, mechanical properties, and bioactivity of bone scaffolds containing calcium silicate. *ScienceAsia* 37, 240–246. doi:10.2306/scienceasia1513-1874.2011.37.240
- Kazemi-Darabadi, S., Nayebzadeh, R., Shahbazfar, A. A., Kazemi-Darabadi, F., and Fathi, E. (2019). Curcumin and nanocurcumin oral supplementation improve muscle healing in a rat model of surgical muscle laceration. *Bull. Emerg. Trauma* 7, 292–299. doi:10.29252/beat-0703013
- Law, K.-Y. (2014). Definitions for hydrophilicity, hydrophobicity, and superhydrophobicity: getting the basics right. *J. Phys. Chem. Lett.* 5, 686. doi:10.1021/jz402762h
- Li, W., Zaloga, J., Ding, Y., Liu, Y., Janko, C., Pischetsrieder, M., et al. (2016). Facile preparation of multifunctional superparamagnetic PHBV microspheres containing SPIONs for biomedical applications. *Sci. Rep.* 6, 23140. doi:10.1038/srep23140
- Liechty, W. B., Kryscio, D. R., Slaughter, B. V., and Peppas, N. A. (2010). Polymers for drug delivery systems. *Annu. Rev. Chem. Biomol. Eng.* 1, 149. doi:10.1146/annurev-chembioeng-073009-100847
- Mahmoudi, M., Simchi, A., Imani, M., Shokrgozar, M. A., Milani, A. S., Hafeli, U. O., et al. (2010). A new approach for the *in vitro* identification of the cytotoxicity of superparamagnetic iron oxide nanoparticles. *Colloids Surfaces B Biointerfaces* 75, 300–309. doi:10.1016/j.colsurfb.2009.08.044
- Masood, F., Chen, P., Yasin, T., Hasan, F., Ahmad, B., and Hameed, A. (2013). Synthesis of poly-(3-hydroxybutyrate-co-12 mol % 3-hydroxyvalerate) by *Bacillus cereus* FB11: its characterization and application as a drug carrier. *J. Mat. Sci. Mat. Med.* 24, 1927–1937. doi:10.1007/s10856-013-4946-x
- Matuszak, J., Dorfler, P., Zaloga, J., Unterweger, H., Lyer, S., Dietel, B., et al. (2015). Shell matters: Magnetic targeting of SPIONs and *in vitro* effects on endothelial and monocytic cell function. *Clin. Hemorheol. Microcirc.* 61, 259–277. doi:10.3233/ch-151998
- Mehrotra, N., Gupta, M., Kovar, A., and Meibohm, B. (2007). The role of pharmacokinetics and pharmacodynamics in phosphodiesterase-5 inhibitor therapy. *Int. J. Impot. Res.* 19, 253–264. doi:10.1038/sj.ijir.3901522
- Mok, H., and Zhang, M. (2013). Superparamagnetic iron oxide nanoparticle-based delivery systems for biotherapeutics. *Expert Opin. Drug Deliv.* 10, 73–87. doi:10.1517/17425247.2013.747507
- Monnier, A., Rombouts, C., Kouider, D., About, I., Fessi, H., and Sheibat-Othman, N. (2016). Preparation and characterization of biodegradable polyhydroxybutyrate-co-hydroxyvalerate/polyethylene glycol-based microspheres. *Int. J. Pharm.* X 513, 49–61. doi:10.1016/j.ijpharm.2016.08.066
- Mutlu, G., Calamak, S., Ulubayram, K., and Guven, E. (2018). Curcumin-loaded electrospun PHBV nanofibers as potential wound-dressing material. *J. Drug Deliv. Sci. Technol.* 43, 185–193. doi:10.1016/j.jddst.2017.09.017
- Naqvi, S., Samim, M., Abdin, M. Z., Ahmad, F. J., Prashant, C. K., Ahmed, A., et al. (2010). Concentration-dependent toxicity of iron oxide nanoparticles mediated by increased oxidative stress. *Int. J. Nanomedicine* 5, 983–989. doi:10.2147/ijn.s13244
- Nguyen, T. T., and Jeong, J. (2018). Development of a single-jet electro spray method for producing quercetin-loaded poly(lactic-co-glycolic acid) microspheres with prolonged-release patterns. *J. Drug Deliv. Sci. Technol.* 47, 268–274. doi:10.1016/j.jddst.2018.07.005
- Nigmatullin, R., Thomas, P., Lukasiewicz, B., Puthussery, H., and Roy, I. (2015). Polyhydroxyalkanoates, a family of natural polymers, and their applications in drug delivery. *J. Chem. Technol. Biotechnol.* 90, 1209–1221. doi:10.1002/jctb.4685
- Panith, N., Assavanig, A., Lertsiri, S., Bergkvist, M., Surarit, R., and Niamsiri, N. (2016). Development of tunable biodegradable polyhydroxyalkanoates microspheres for controlled delivery of tetracycline for treating periodontal disease. *J. Appl. Polym. Sci.* 133. doi:10.1002/app.44128
- Parodi, A., Quattrocchi, N., van de Ven, A. L., Chiappini, C., Evangelopoulos, M., Martinez, J. O., et al. (2013). Synthetic nanoparticles functionalized with biomimetic leukocyte membranes possess cell-like functions. *Nat. Nanotechnol.* 8, 61–68. doi:10.1038/nnano.2012.212
- Patil, R. M., Thorat, N. D., Shete, P. B., Bedge, P. A., Gavde, S., Joshi, M. G., et al. (2018). Comprehensive cytotoxicity studies of superparamagnetic iron oxide nanoparticles. *Biochem. Biophys. Rep.* 13, 63–72. doi:10.1016/j.bbrep.2017.12.002
- Pérez-Arauz, A. O., Aguilar-Rabiela, A., Vargas-Torres, A., Rodriguez-Hernandez, A. I., Chavarria-Hernandez, N., Vergara-Porras, B., et al. (2019). Production and characterization of biodegradable films of a novel polyhydroxyalkanoate (PHA) synthesized from peanut oil. *Food Packag. Shelf Life* 20, 100297. doi:10.1016/j.fpsl.2019.01.001
- Pulido-Moran, M., Moreno-Fernandez, J., Ramirez-Tortosa, C., and Ramirez-Tortosa, M. (2016). Curcumin and health. *Molecules* 21, 264. doi:10.3390/molecules21030264
- Qi, L., Jiang, J., Zhang, J., Zhang, L., and Wang, T. (2020). Curcumin protects human trophoblast HTR8/SVneo cells from H₂O₂-induced oxidative stress by activating Nrf2 signaling pathway. *Antioxidants* 9, 121. doi:10.3390/antiox9020121
- Rahaman, M. S., Banik, S., Akter, M., Rahman, M. M., Sikder, M. T., Hosokawa, T., et al. (2020). Curcumin alleviates arsenic-induced toxicity in PC12 cells via modulating autophagy/apoptosis. *Ecotoxicol. Environ. Saf.* 200, 110756. doi:10.1016/j.ecoenv.2020.110756
- Rahimnia, R., Salehi, Z., Ardestani, M. S., and Doosthoseini, H. (2019). SPION conjugated curcumin nano-imaging probe: Synthesis and bio-physical evaluation. *Iran. J. Pharm. Res.* 18, 183–197.
- Senthilkumar, P., Dawn, S., Sree Samanvitha, K., Sanjay Kumar, S., Narendra Kumar, G., and Samrot, A. V. (2017). Optimization and characterization of poly[R]

hydroxyalkanoate of *Pseudomonas aeruginosa* SU-1 to utilize in nanoparticle synthesis for curcumin delivery. *Biocatal. Agric. Biotechnol.* 12, 292–298. doi:10.1016/j.bcab.2017.10.019

Si, J.-C., Xing, Y., Peng, M. L., Zhang, C., Buske, N., Chen, C., et al. (2013). Solvothermal synthesis of tunable iron oxide nanorods and their transfer from organic phase to water phase. *CrystEngComm* 16, 512–516. doi:10.1039/c3ce41544a

Singh, N., Jenkins, G. J. S., Asadi, R., and Doak, S. H. (2010). Potential toxicity of superparamagnetic iron oxide nanoparticles (SPION). *Nano Rev.* 1, 5358. doi:10.3402/nano.v1i0.5358

Sodipo, B. K., Abdul, A., Letter, A., Bashiru, E., and Sodipo, K. (2014). A sonochemical approach to the direct surface functionalization of superparamagnetic iron oxide nanoparticles with (3-aminopropyl) triethoxysilane. *Beilstein J. Nanotechnol.* 5, 1472–1476. doi:10.3762/bjnano.5.160

Solar, P., Gonzalez, G., Vilos, C., Herrera, N., Juica, N., Moreno, M., et al. (2015). Multifunctional polymeric nanoparticles doubly loaded with SPION and ceftiofur retain their physical and biological properties. *J. Nanobiotechnology* 13, 14–12. doi:10.1186/s12951-015-0077-5

Tietze, R., Zaloga, J., Janko, C., Lyer, S., Unterweger, H., Friedrich, R. P., et al. (2015). Magnetic nanoparticle-based drug delivery for cancer therapy. *Biochem. Biophys. Res. Commun.* 468, 463. doi:10.1016/j.bbrc.2015.08.022

Vakili-Ghartavol, R., Momtazi-Borojeni, A. A., Vakili-Ghartavol, Z., Aiyelabegan, H. T., Jaafari, M. R., Rezayat, S. M., et al. (2020). Toxicity assessment of superparamagnetic iron oxide nanoparticles in different tissues. *Artif. Cells Nanomed. Biotechnol.* 48, 443–451. doi:10.1080/21691401.2019.1709855

Van Nong, H., Hung, L. X., Thang, P. N., Chinh, V. D., Vu, L. V., Dung, P. T., et al. (2016). Fabrication and vibration characterization of curcumin extracted from turmeric (*Curcuma longa*) rhizomes of the northern Vietnam. *Springerplus* 5, 1147. doi:10.1186/s40064-016-2812-2

Wei, Z., Chen, L., Thompson, D. M., and Montoya, L. D. (2012). Effect of particle size on *in vitro* cytotoxicity of titania and alumina nanoparticles. *J. Exp. Nanosci.* 9, 1. doi:10.1080/17458080.2012.683534

Wei, Z., Chen, L., Thompson, D. M., and Montoya, L. D. (2014). Effect of particle size on *in vitro* cytotoxicity of titania and alumina nanoparticles. *J. Exp. Nanosci.* 9, 625–638. doi:10.1080/17458080.2012.683534

Zaloga, J., Janko, C., Nowak, J., Matuszak, J., Knap, S., Eberbeck, D., et al. (2014). Development of a lauric acid/albumin hybrid iron oxide nanoparticle system with improved biocompatibility. *Int. J. Nanomedicine* 9, 4847–4866. doi:10.2147/ijn.s68539

Zhan, X., Dai, L., Zhang, L., and Gao, Y. (2020). Entrapment of curcumin in whey protein isolate and zein composite nanoparticles using pH-driven method. *Food Hydrocoll.* 106, 105839. doi:10.1016/j.foodhyd.2020.105839

Zhi, D., Yang, T., Yang, J., Fu, S., and Zhang, S. (2020). Targeting strategies for superparamagnetic iron oxide nanoparticles in cancer therapy. *Acta Biomater.* 102, 13–34. doi:10.1016/j.actbio.2019.11.027

Zidan, A. S., Rahman, Z., and Khan, M. A. (2011). Product and process understanding of a novel pediatric anti-HIV tenofovir niosomes with a high-pressure homogenizer. *Eur. J. Pharm. Sci.* 44, 93–102. doi:10.1016/j.ejps.2011.06.012